Primordial density and BAO reconstruction

Hong-Ming Zhu,[1,2] Ue-Li Pen,[3,4,5,6] Matthew McQuinn,[7] and Xuelei Chen[1,2,8]

[1]*Key Laboratory for Computational Astrophysics, National Astronomical Observatories, Chinese Academy of Sciences, 20A Datun Road, Beijing 100012, China*
[2]*University of Chinese Academy of Sciences, Beijing 100049, China*
[3]*Canadian Institute for Theoretical Astrophysics, University of Toronto, 60 St. George Street, Toronto, Ontario M5S 3H8, Canada*
[4]*Dunlap Institute for Astronomy and Astrophysics, University of Toronto, 50 St. George Street, Toronto, Ontario M5S 3H4, Canada*
[5]*Canadian Institute for Advanced Research, CIFAR Program in Gravitation and Cosmology, Toronto, Ontario M5G 1Z8, Canada*
[6]*Perimeter Institute for Theoretical Physics, 31 Caroline Street North, Waterloo, Ontario, N2L 2Y5, Canada*
[7]*Department of Astronomy, University of Washington, Seattle, WA 98195, USA*
[8]*Center of High Energy Physics, Peking University, Beijing 100871, China*

(Dated: August 26, 2016)

In this paper we introduce a new way to reconstruct BAO peaks in real space. ..... how to briefly summarize this?

PACS numbers:

I. INTRODUCTION

do we need to add more content before the first paragraph?

The standard BAO reconstruction uses the negative Zel'dovich (linear) displacement to reverse the large-scale bulk flows [1]. The nonlinear density field is usually smoothed on the linear scale (~ 10 Mpc$/h$) to make the Zel'dovich approximation valid. Actually, the fully nonlinear displacement which describes the motion beyond the linear order (the Zel'dovich approximation) can be solved from the nonlinear density field. While the algorithm is complicated in the three spatial dimensions, it is quite simple in the 1D case, which is basically the ordering of mass elements. The 1D cosmological dynamics corresponds to the interaction of infinite sheets of matter where the force is independent of distance [2]. These sheets are moving in a Hubble flow relative to one another and the surface density in each sheet scales as a^{-2}. The simplified 1D dynamics provides an excellent means of understanding the structure formation and testing perturbation theories [2]. In this paper we solve the fully nonlinear displacement in 1D and present a new method to reconstruct the primordial density field and hence the linear BAO information.

This paper is organized as follows. In Section II, we briefly describe the 1D N-body simulation. In Section III, we present the reconstruction algorithm in the 1D case. In Section IV, we show the results of reconstruction. In Section V, we discuss the 3D case and future improvements.

II. SIMULATIONS

To simulate the gravitational dynamics in 1D, we use the 1D particle-mesh (PM) code in Ref. [2]. The 1D simualtion we use involves 3×10^8 sheets with 3×10^8 PM elements in a 10^8 Mpc box. The initial condition is generated using the Zel'dovich approximation. Since the Zel'dovich approximation is exact up to shell crossing, we start the PM calculation at $z = 10$. In the analysis, we use the output at $z = 0$. We scale the initial density field by the linear growth factor to get the linear density field at $z = 0$.

III. RECONSTRUCTION ALGORITHM

The Lagrangian displacement $\Psi(q)$ fully describes the motion of mass elements. The Eulerian position x of a mass element is

$$x = q + \Psi(q), \tag{1}$$

where q is the initial Lagrangian position of this mass element. In the simulations, mass elements (sheets) are labeled by their initial Lagrangian coordinates. Once we know their Eulerian positions, the displacment field is obtained. Observationally, we only have the unlabelled Eulerian coordinates. The estimated displacement at the Lagrangian coordinate $q = iL/N$ is

$$s(q) = x_i - iL/N, \tag{2}$$

where we have ordered the sheet lables i from left to right, L is the box size, and N is the sheet number. If no shell crossing happens, the reconstructed displacement is exact up to a global shift. In the nonlinear regime once shell crossing occurs, the estimated displacement field is quite noisy on the scale $\sim L/N$. To reduce stochasticities in the estimated displacement field, we can use the averaged displacement of n_p particles

$$s(q) = \frac{1}{n_p} \sum_{j=i}^{i+n_p-1} x_j - in_pL/N, \tag{3}$$

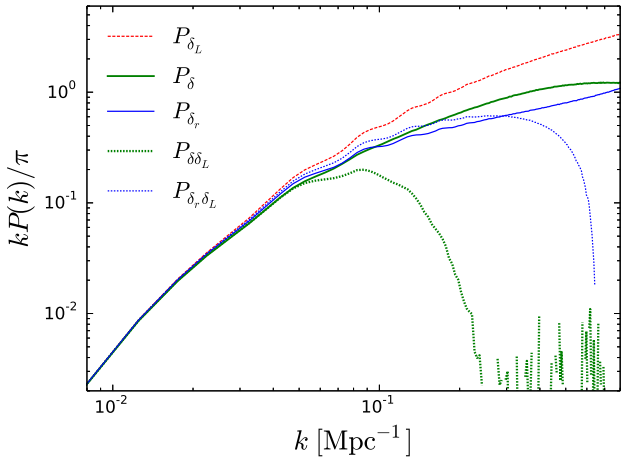

FIG. 1: The power spectra of the linear (dashed line), nonlinear (thick solid line), and reconstructed (thin solid line) fields. We also plot the nonlinear-linear (thick dotted line) and reconstructed-linear (thin dotted line) cross-correlation power spectra. The wiggles in the reconstructed power spectrum are also much more transparent than the nonlinear power spectrum.

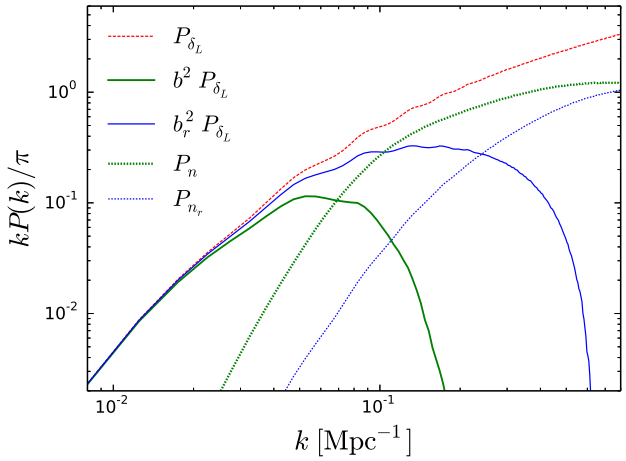

FIG. 2: The linear power spectrum (dashed line), the linear components in the nonlinear (thick solid line) and reconstructed (thin solid line) fields, the noise parts of the nonlinear (thick dotted line) and reconstructed (thin dotted line) fields. The noise terms dominate over the signals at $k \gtrsim 0.07$ Mpc^{-1} for the nonlinear field and $k_q \gtrsim 0.24$ Mpc^{-1} for the reconstructed field.

where $q = in_pL/N$ and j is the sheet label. Here i varies from 0 to N/n_p and j varies from 0 to N. We take $n_p = 5$ to estimate the displacement field in this paper.

The derivative (actually the divergence) of $s(q)$ gives the reconstructed density field

$$\delta_r(q) = -\frac{\partial s(q)}{\partial q}, \tag{4}$$

i.e., the differential motion of mass elements. is this argument appropriate? shall we discuss more here? Reconstruction from the gridded density field can be implemented following the same principle, which we adopt in the following calculations.

IV. RESULTS

Figure 1 shows the linear, nonlinear and reconstructed power spectra, as well as the cross-corrlation power spectra. The correlation of the reconstruction density field δ_r with the linear density field δ_L is much better than that of the raw nonlinear density field δ. The wiggles in the reconstructed power spectrum are also much more apparent than the nonlinear power spectrum. The nonlinear density field $\delta(x)$ is given on the Eulerian position x, while the reconstructed density field $\delta_r(q)$ is calculated on the Lagrangian position q.

To convenienty quantify the linear information δ_L in the nonlinear density field δ, we decompose the nonlinear density field δ as

$$\delta(k) = b(k)\delta_L(k) + n(k). \tag{5}$$

Here, $b\delta_L$ is completely correlated with the linear density field δ_L. Correlating the nonlinear density field with the linear density field,

$$\langle\delta(k)\delta_L(k)\rangle = b(k)\langle\delta_L(k)\delta_L(k)\rangle, \tag{6}$$

we obtain

$$b(k) = \frac{P_{\delta\delta_L}(k)}{P_{\delta_L}(k)}. \tag{7}$$

Nonlinear evolution drives b to drop from unity, reducing the linear signal. Separating the part correlated with the linear density field, we then have $n(k) = \delta(k) - b(k)\delta_L(k)$. n is generated in the nonlinear evolution and thus uncorrelated with the linear density field δ_L, further reducing $b\delta_L$ with respect to δ. This part induces noise in the measurement of BAO. Such decomposition helps to write the nonlinear power spectrum as

$$P_\delta(k) = b^2(k)P_{\delta_L}(k) + P_n(k). \tag{8}$$

Here, $b(k)$ is often referred as the "propagator" and P_n is usually called the mode-coupling term [3–5]. For the reconstructed field $\delta_r(q)$, we also have

$$\delta_r(k_q) = b_r(k_q)\delta_L(k_q) + n_r(k_q), \tag{9}$$

where

$$b_r(k_q) = \frac{P_{\delta_r\delta_L}(k_q)}{P_{\delta_L}(k_q)}. \tag{10}$$

The reconstructed power specrum is

$$P_{\delta_r}(k_q) = b_r^2(k_q)P_{\delta_L}(k_q) + P_{n_r}(k_q). \tag{11}$$

Here, the subscript "q" denotes that the reconstructed field is given on the Lagraigian coordinate. In Fig. 2 we

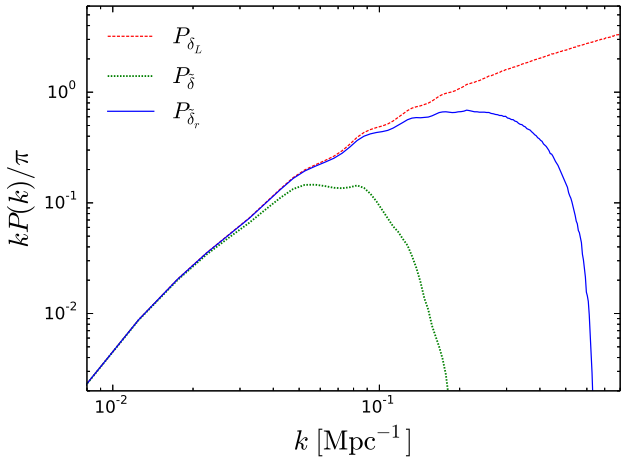

FIG. 3: The power spectra for the linear (dashed line), filtered nonlinear (dotted line) and filtered reconstructed (solid line) fields.

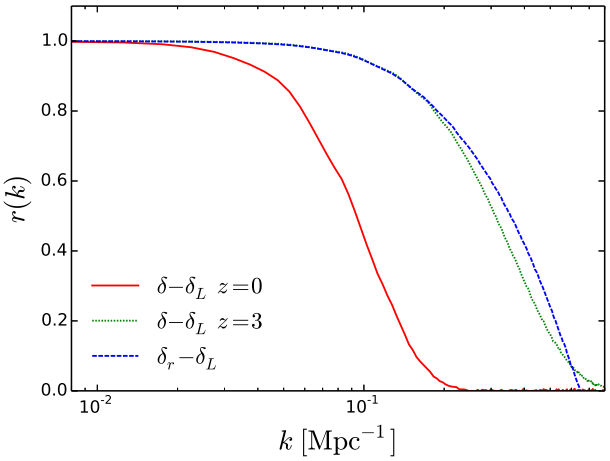

FIG. 5: The $\delta - \delta_L$ correlation coefficients at $z = 0$ (solid line) and $z = 3$ (dotted line), as well as the $\delta_r - \delta_L$ correlation coefficient (dashed line).

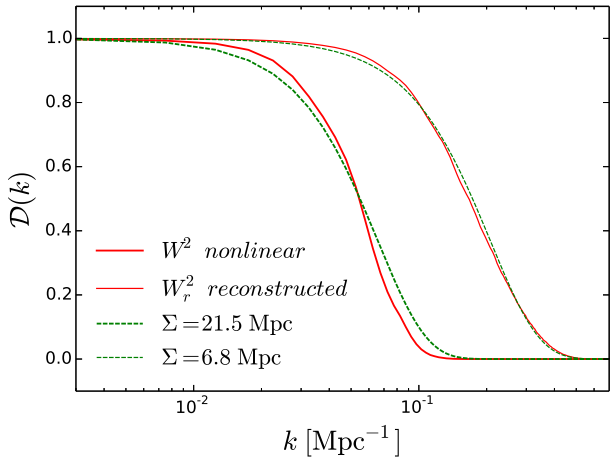

FIG. 4: The damping factors for the nonlinear (thick solid line) and reconstructed (thin solid line) fields. The Gaussian BAO damping models with $\Sigma = 21.5$ Mpc (thick dashed line) and $\Sigma = 6.8$ Mpc (thin dashed line).

plot the linear components and the noise terms of the nonlinear and reconstructed fields.

The raw reconstructed field δ_r is still noisy on small scales ($k_q \gtrsim 0.24$ Mpc^{-1}). To optimally filter out the noise from the raw reconstructed field, we use the Wiener filter

$$W_r(k_q) = \frac{P_{\delta_L}(k_q)}{P_{\delta_L}(k_q) + P_{n_r}(k_q)/b_r^2(k_q)}. \quad (12)$$

Deconvolving b_r and using the Wiener filtering, we obtain the optimal reconstructed field,

$$\tilde{\delta}_r(k_q) = \frac{\delta_r(k_q)}{b_r(k_q)} W_r(k_q). \quad (13)$$

The power spectrum of the optimal reconstructed field $\tilde{\delta}_r$ is given by

$$P_{\tilde{\delta}_r}(k_q) = W_r^2(k_q) P_{\delta_L}(k_q) + W_r^2(k_q) P_{n_r}(k_q)/b_r^2(k_q), \quad (14)$$

where W_r^2 describes the dampling of the linear power spectrum. The suppression of the linear power spectrum by b^2 can be fully corrected if P_n is zero, while the damping due to W_r^2 can not. The raw nonlinear field δ is also filtered. In Fig. 3, we plot the power spectra of the optimal reconstructed and nonlinear fields.

Figure 4 shows the damping factors for the optimal filtered nonlinear and reconstructed fields. The damping of the linear power spectrum is significantly reduced after reconstruction. We also overplot the best-fitting Gaussian BAO damping model,

$$\mathcal{D}(k) = \mathrm{e}^{-k^2\Sigma^2/2}, \quad (15)$$

with $\Sigma = 21.5$ Mpc and 6.8 Mpc for the nonlinear and reconstructed fields. The new BAO reconstruction algorithm reduces the the nonlinear damping scale Σ by 68 per cent, i.e., a factor of three. The damping factor for the reconstructed field is above 0.8 for $k \lesssim 0.1$ Mpc^{-1}. However, the 100 per cent reconstruction, cancelling any nonlinear effects, is still unachievable, as some information has been irreversibly lost.

Reconstruction reduces the nonlinear damping $\mathcal{D}$ as well as the noise term P_n. To quantify the overall performance, we can use the cross-correltion coefficient

$$r(k) = \frac{P_{\delta\delta_L}(k)}{\sqrt{P_\delta(k) P_{\delta_L}(k)}} = \frac{1}{\sqrt{1+\eta(k)}}, \quad (16)$$

where $\eta = P_n/(b^2 P_{\delta_L})$ quantifies the relative amplitude of n with respect to $b\delta_L$. We plot the cross-correlation coefficients in Fig. 5. The correlation of δ_r with δ_L is even better than that of δ at $z = 3$.

The density fluctuation probability distribution function (PDF) quantifies the Gaussianity of the density field.

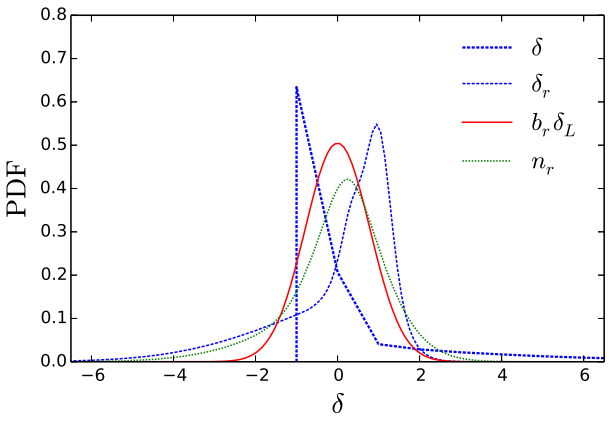

FIG. 6: The probability distribution functions of the nonlinear (thick dashed line) and reconstructed (thin dashed line) fields. We also show the probability distribution functions of the linear component (solid line) and the noise part (dotted line).

Figure 6 shows the PDFs of the nonlinear and reconstructed density fields. We also plot the PDFs of the linear component $b_r\delta_L$ and the noise part n_r of the reconstructed density field δ_r. Of course the linear component is Gaussian, while the noise part is nonGaussian. As a result, the reconstructed density field is also nonGaussian. The raw nonlinear density field is significantly nonGaussian.

V. DISCUSSIONS

The new reconstruction method successfully recovers the lost linear information on the mildly nonlinear scales (till $k \lesssim 0.24$ Mpc^{-1}). The result in 1D provides an intuitive view of the algorithm and motivates us to develop the reconstruction method in 3D. The nonlinear displacement beyond the Zel'dovich approximation in 3D can be solved using the multigrid iteration scheme [6]. The algorithm for solving the 3D nonlinear displacement is originally introduced for the adaptive particle-mesh N-body code [6] and the moving mesh hydrodynamic code [7]. The 3D case is also more complicated since the 3D displacement field involves a curl part (vorticity) which is generated after shell crossing, while this does not happen after particles cross over in 1D. This requires us to quantify the effect of vorticity, which can be accomplished using N-body simulations. By decomposing the simulated displacement field into a irrotational part and a curl part, we can study the statistical properties of different components [8, 9]. These will be presented in future.

The reconstructed nonlinear displacement field is also improtant for the current BAO reconstruction [1], where the linear continuity equation is adopted to solve the displacement under the Zel'dovich approximation. However, the nonlinear displacement retains much more information, describing the motion of dark matter fluid elements beyond the linear order. The reconstructed displacement field $s(q)$ is given on the Lagrangian coordinate instead of the final Eulerian coordinate. This helps to correct the effect due to the use of $s(x)$ instead of $s(q)$ in the BAO reconstruction [10, 11]. As more nonlinear effects will be removed using the nonlinear displacement, we expect the modeling of the reconstructed density field will be simplified.

The Wiener filter is optimal for the case both the signal and the noise are Gaussian random fields. In Fig. 6, the PDFs of the reconstructed density field and the noise are apparently nonGaussian. The reconstruction can be further improved using the nonlinear filtering rather than the Wiener fieltering [12]. We plan to study this in future.

VI. ACKNOWLEDGEMENT

We thank Yu Yu and Tian-Xiang Mao for helpful discussions. We acknowledge the support of the Chinese MoST 863 program under Grant No. 2012AA121701, the CAS Science Strategic Priority Research Program XDB09000000, the NSFC under Grant No. 11373030, IAS at Tsinghua University, and NSERC. The Dunlap Institute is funded through an endowment established by the David Dunlap family and the University of Toronto. Research at the Perimeter Institute is supported by the Government of Canada through Industry Canada and by the Province of Ontario through the Ministry of Research & Innovation.

[1] D. J. Eisenstein, H.-J. Seo, E. Sirko, and D. N. Spergel, ApJ **664**, 675 (2007), astro-ph/0604362.
[2] M. McQuinn and M. White, J. Cosmology Astropart. Phys. **1**, 043 (2016), 1502.07389.
[3] M. Crocce and R. Scoccimarro, Phys. Rev. D **73**, 063520 (2006), astro-ph/0509419.
[4] M. Crocce and R. Scoccimarro, Phys. Rev. D **77**, 023533 (2008), 0704.2783.
[5] T. Matsubara, Phys. Rev. D **77**, 063530 (2008), 0711.2521.
[6] U.-L. Pen, ApJS **100**, 269 (1995).
[7] U.-L. Pen, ApJS **115**, 19 (1998), astro-ph/9704258.
[8] P. Zhang, J. Pan, and Y. Zheng, Phys. Rev. D **87**, 063526 (2013), 1207.2722.
[9] Y. Zheng, P. Zhang, Y. Jing, W. Lin, and J. Pan, Phys. Rev. D **88**, 103510 (2013), 1308.0886.
[10] M. White, MNRAS **450**, 3822 (2015), 1504.03677.
[11] M. Schmittfull, Y. Feng, F. Beutler, B. Sherwin, and M. Y. Chu, Phys. Rev. D **92**, 123522 (2015), 1508.06972.
[12] U.-L. Pen, Philosophical Transactions of the Royal Society of London Series A **357**, 2561 (1999), astro-ph/9904170.